

Electrochemical studies of Mn_3HgM ($M = Mo, W, Mn, Fe$ or Co) and Mn_3Au cluster anions

Oriol Rossell ^{a,*}, Miquel Seco ^a, Glòria Segalés ^a, René Mathieu ^b,
Dominique de Montauzon ^b

^a *Departament de Química Inorgànica, Universitat de Barcelona, Diagonal 647, E-08028 Barcelona, Spain*

^b *Laboratoire de Chimie de Coordination du CNRS, 205 Route Narbonne, 31077 Toulouse Cedex, France*

Received 22 May 1995

Abstract

The electrochemical behaviour of compounds of the type $(PPh_4)[Mn_3(CO)_{12}(\mu_3-H)(\mu-Hgm)]$ [$m = Mo(CO)_3Cp$ (1), $W(CO)_3Cp$ (2), $Mn(CO)_5$ (3), $Fe(CO)_2Cp$ (4) or $Co(CO)_4$ (5)] and the $[PPh_4]^+$ salts of the anions $[(Mn_3(CO)_{12}(\mu_3-H)_2Hg)]^{2-}$ (6), $[(Mn_3(CO)_{12}(\mu_3-H)Au)_2(dppe)]^{2-}$ (7) and $[(Mn_3(CO)_{12}(\mu_3-H)Au)_n(triphos)(AuCl)_{3-n}]^{n-}$ [$n = 1$ (8), 2(9), 3(10)] has been investigated at Pt (or Au) electrodes in CH_2Cl_2 or THF by means of cyclic voltammetry and coulometry. All the compounds undergo a quasi-reversible oxidation and an irreversible reduction. The electrons involved in both oxidation and reduction are delocalized mainly onto the metal fragments, Mn_3Hg and Mn_3Au , and the slight changes in the redox potential throughout the series of compounds are explained in terms of the nucleophilicity of the metal fragments, m . In the series of gold clusters a weak electronic interaction has been observed between the metal units through the triphosphine.

Keywords: Manganese; Mercury; Gold; Electrochemistry; Cluster

1. Introduction

Cluster electrochemistry is a field of growing interest, with many possible applications both in electrosynthesis and electrocatalysis. Homonuclear clusters have been studied more extensively than heteronuclear, since the latter exhibit more complex electrochemical behaviour [1]. There are only a few reports concerning mercury- or gold-containing transition-metal clusters [2,3]. Recently, we described the electrochemical oxidation of the iron compounds $[PPh_4][Fe_3(CO)_{11}(\mu-Hgm)]$ [$m =$ metal fragment, such as $Mo(CO)_3Cp$] [2c] and were able to detect the paramagnetic species $[Fe_3(CO)_{11}(\mu-Hgm)]^+$ by EPR spectroscopy. These results prompted us to investigate the electrochemical behaviour of the isoelectronic manganese compounds $[PPh_4][Mn_3(CO)_{12}(\mu_3-H)(\mu-Hgm)]$ [4] in an attempt to compare the two series of derivatives. Unfortunately, although an oxidation process was evident for all the compounds, no radical species were ever detected. However, a detailed study of the electrochemical reduc-

tion of these compounds by cyclic voltammetry and coulometry has helped to clarify some aspects of the pathways for reductive cleavage of the mercury–manganese bond. Moreover, considering the isolobal relationship between Hgm^+ and $AuPR_3^+$, we extended this study to the family of gold derivatives $[(Mn_3(CO)_{12}(\mu_3-H)Au)_n(triphos)(AuCl)_{3-n}]^{n-}$ [5], to determine whether there is any electronic interaction between different Mn_3Au fragments via the triphosphine.

2. Results and discussion

2.1. Electrochemical behaviour of the clusters $[PPh_4][Mn_3(CO)_{12}(\mu_3-H)(\mu-Hgm)]$

The electrochemical properties of $[PPh_4][Mn_3(CO)_{12}(\mu_3-H)(\mu-Hgm)]$ [$m = Mo(CO)_3Cp$ (1), $W(CO)_3Cp$ (2), $Mn(CO)_5$ (3), $Fe(CO)_2Cp$ (4) or $Co(CO)_4$ (5)] [4] — the anionic structure of which is shown in Fig. 1 — were studied in the electroactivity range of dichloromethane on a Pt disk electrode at $-10^\circ C$ in order to prevent their decomposition. All cyclic voltammograms at $0.1 V s^{-1}$ exhibit: (i) an oxidation wave at about 0.40 V vs. SCE, quasi-reversi-

* Corresponding author.

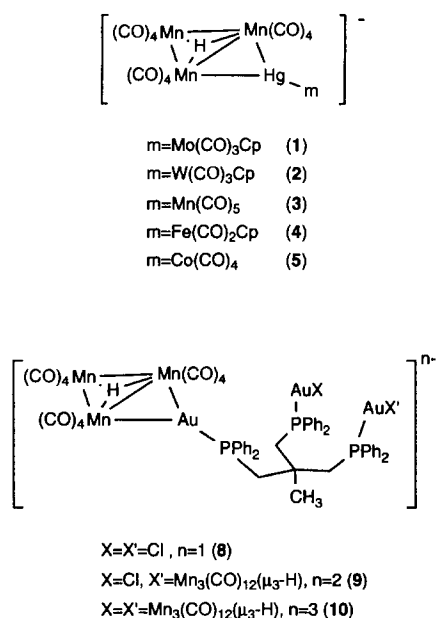
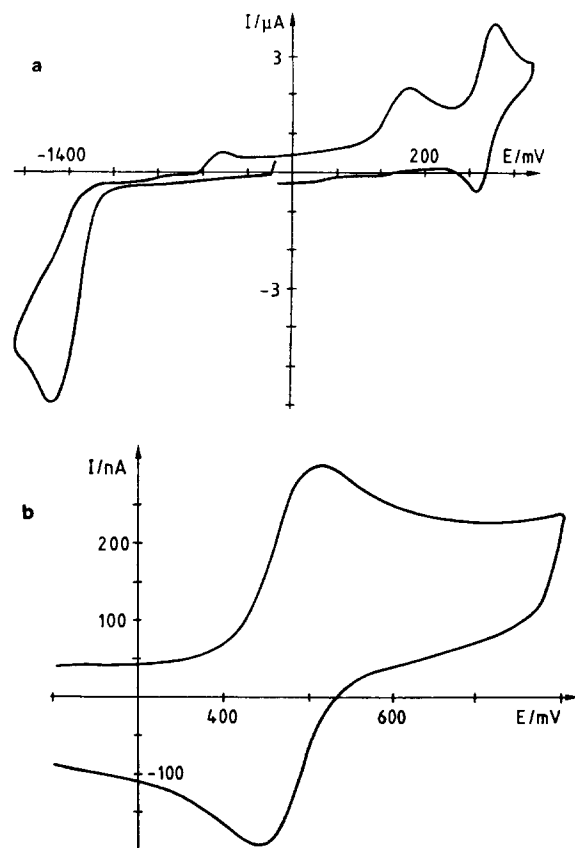


Fig. 1. Schematic structure of the anions 1–5 and 8–10.

ble at high scan rates; (ii) two irreversible oxidation peaks at about 0.8 and 1.2 V; and (iii) an irreversible reduction process at about -1.5 V.

The waves at 0.40 V (Fig. 2) appeared quasi-reversible at different scan rates. For instance, at 0.1 V s^{-1} when $m = \text{Mn}(\text{CO})_5$, the intensity ratio $i_{p,c}/i_{p,a}$ was 0.5, for **5** it was only 0.3 and for **4** no return peak was observed. The quasi-reversibility indicates that this oxidation step is followed by a relatively fast chemical reaction. Standard potentials obtained at 50 V s^{-1} using a Technic ultramicroelectrode are summarized in Table 1. The electron-transfer rate constants k^0 calculated by the Nicholson and Shain method [6] were about $10^{-1} \text{ cm s}^{-1}$, typical of a pseudo-reversible process. The transfer coefficients α were 0.5–0.6.

The linear voltammograms at a rotating Pt disk electrode indicated some passivation (for **1** the study was performed on an Au electrode) and the plot of limiting current versus the square root of the electrode rotation

Fig. 2. Cyclic voltammogram of compound **5**, (a) at 0.5 V s^{-1} and (b) the quasi-reversible wave at 50 V s^{-1} .

speed showed a deviation from linearity corresponding to a diffusion-controlled process.

Controlled-potential coulometry at 0.7 V using a Pt gauze at -10°C and at -40°C in dichloromethane with $[\text{nBu}_4\text{N}][\text{PF}_6]$ as the supporting electrolyte indicated that one electron was transferred, but that the radical generated rapidly decomposed. The dark green solutions became green–yellow in colour and their frozen-glass EPR spectra showed no signal, even at liquid He temperature. The estimated lifetimes [6] for these compounds are a few seconds. All oxidized solutions showed the same $\nu(\text{CO})$ pattern in the IR spectrum — which

Table 1
Electrochemical data for the oxidation step of complexes 1–5^a

Compound	m	E^0 (V)	$E_{p,a} - E_{p,c}$ (mV)	$i_{p,c}/i_{p,a}$	n
1 ^b	$\text{Mo}(\text{CO})_3\text{Cp}$	0.42	80	0.79	1
2	$\text{W}(\text{CO})_3\text{Cp}$	0.35	58	0.78	1
3	$\text{Mn}(\text{CO})_5$	0.41	64	0.75	1
4	$\text{Fe}(\text{CO})_2\text{Cp}$	0.30	77	0.69	1
5	$\text{Co}(\text{CO})_4$	0.48	58	0.80	1

^a Cyclic voltammetry at -10°C in dichloromethane 0.1 M $[\text{nBu}_4\text{N}][\text{PF}_6]$ at 50 V s^{-1} ; working electrode Pt ($r = 100 \mu\text{m}$); potentials vs. SCE.

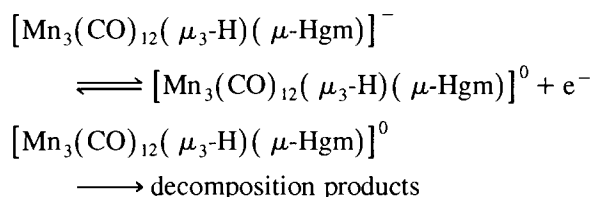
^b Working electrode Au ($r = 125 \mu\text{m}$).

Table 2
Reduction data for complexes 1–5^a

Cluster	m	$E_{p,r}$ (V)	n	E_{p1} (V)	E_{p2} (V)
1	Mo(CO) ₃ Cp	-1.46	2	-0.25	-0.09
2	W(CO) ₃ Cp	-1.47	2	-0.25	-0.06
3	Mn(CO) ₅	-1.45	2	-0.25	(-0.25)
4	Fe(CO) ₂ Cp	-1.61	2	-0.25	-0.95
5	Co(CO) ₄	-1.45	2	-0.25	+0.20

^a Cyclic voltammetry values obtained in dichloromethane 0.1 M [ⁿBu₄N][PF₆], scan rate 0.1 V s⁻¹; working electrode Pt (*d* = 1 mm); potentials vs. SCE.

could not be assigned — with bands at 2085 (w); 2056–2059 (m); 2045 (w); 2029 (m); 2009 (s); 1990 (vs); 1951 (m); 1933 (m) cm⁻¹, suggesting that only slight changes had occurred. These results clearly show that the first redox couple corresponds to a simple monoelectronic process as follows,



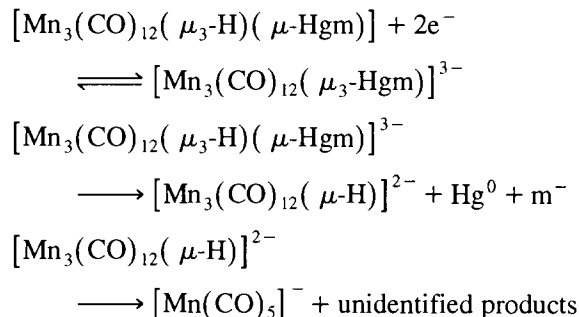
The other oxidation steps were not studied further.

The intensity of the irreversible reduction wave at -1.5 V was double that of the oxidation wave at 0.40 V. The fact that a small reverse peak is observed at higher scan rates and that in the reverse scan some additional peaks appeared at scan rates of 1 V s⁻¹ (Table 2) indicates that the electrochemical step is followed by a chemical reaction. All result from the reduction process, as confirmed by pre-electrolysis cyclic voltammograms. The peak E_{p1} at -0.25 V was attributed to the oxidation of the anion $[\text{Mn}(\text{CO})_5]^-$ by comparison with literature values [7a,b] and confirmed by cyclic voltammetry of an authentic sample under the same conditions. The E_{p2} peaks correspond to the oxidation of m^- fragments and were identified by comparison with literature data [2c,7]. Other peaks appeared at -0.40 V and -0.60 V for complex 4, and at -0.40 V and -0.70 V for complex 5. The quasi-reversible oxidation wave at -0.40 V was characterized as the one-electron oxidation of $[\text{Mn}_3(\text{CO})_{12}(\mu\text{-H})]^{2-}$ leading to $[\text{Mn}(\text{CO})_5]^-$ and $[\text{Mn}_2(\text{CO})_{10}]$. Other peaks could not be assigned.

Exhaustive controlled-potential electrolysis at -1.70 V consumed two electrons per mole. IR spectroscopy of the resulting brown–green solutions confirmed the formation of species m^- . Another unidentified species also appeared, with bands at 1957 (s) and 1934 (m) cm⁻¹. In the case of $m = \text{Fe}(\text{CO})_2\text{Cp}$ (4), the electrolysis was faster than for complexes 1–3 and 5 and the dianion $[\text{Mn}_3(\text{CO})_{12}(\mu\text{-H})]^{2-}$ was detected by IR spectroscopy although, surprisingly, under these conditions it rapidly

decomposed. We suggest that $[\text{Mn}_3(\text{CO})_{12}(\mu\text{-H})]^{2-}$ may be formed in all cases but that it decomposes before being detected.

From these data we propose the following mechanism, which is similar to those found for mHgm compounds [2a], $[\text{Ru}_3(\text{CO})_9(\mu_3\text{-}\eta^2\text{-C}\equiv\text{C}'\text{Bu})\text{Hg}(\text{Mo}(\text{CO})_3\text{Cp})]$ [2b] and $[\text{Fe}_3(\text{CO})_{11}(\mu\text{-Hgm})]^-$ [2c]:



Tables 1 and 2 show that the iron derivative 4 is the easiest to oxidize and consequently the most difficult to reduce. Derivative 5 exhibits the converse behaviour, as observed for the analogous spiked butterfly metal clusters with an Fe₃Hgm core [2c]. Values obtained for compounds 1, 2 and 3 are intermediate between those of 4 and 5. These trends can be explained in terms of the

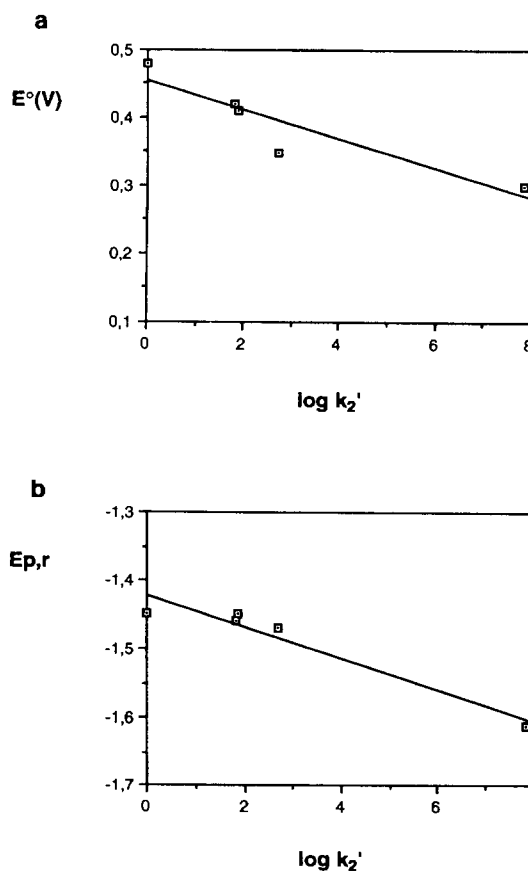


Fig. 3. Plot of voltammetry potentials (a) E° ($r = 0.87$) and (b) $E_{p,r}$ for reduction ($r = 0.92$), versus $\log k_2'$.

nucleophilicity of the corresponding carbonylmetallate anions m^- , which follow the sequence $\text{Fe}(\text{CO})_2\text{Cp} \gg \text{W}(\text{CO})_3\text{Cp} > \text{Mn}(\text{CO})_5 > \text{Mo}(\text{CO})_3\text{Cp} > \text{Co}(\text{CO})_4$ [8]. Thus, there is a strong correlation between the basicity of the $\text{Mn}_3\text{Hg}m$ skeletons, which increases along the series from **5** to **4**, and the ease of cluster reduction and oxidation. These findings are represented graphically in Fig. 3(a), where the plot of E^0 vs. $\log k'_2$, taken as a measure of the nucleophilicity of the metal anions [8], is shown. The same behaviour is observed for the plot of $E_{p,r}$ vs. $\log k'_2$, although $E_{p,r}$ is not a thermodynamic parameter [Fig. 3(b)].

Remarkably, the similar oxidation and reduction potentials for the five compounds (the largest differences being 0.18 and 0.16 V, respectively) indicates that electronic exchange occur in molecular orbitals localized mostly on the Mn_3Hg core. In fact, orbital molecular calculations carried out on $[\text{PPh}_4][\text{Mn}_3(\text{CO})_{12}(\mu_3\text{-H})(\mu\text{-Hg}m)]$ [4] have shown that the frontier orbital LUMO, involved in the reduction process, and the HOMO orbital involved in the oxidation step, are Mn_3Hg -based antibonding and Mn_3 -based bonding orbitals, respectively. Consequently, both electrochemical reduction and oxidation processes tend to weaken the metal skeleton. These results are consistent with those reported for the compounds $[\text{Fe}_3(\text{CO})_{11}(\mu\text{-Hg}m)]^-$ [2c], for which EPR studies after oxidation showed that the m fragment was not involved in the delocalization of the unpaired electron. The different stability of the radical species in either case probably arises from the different stabilities of the starting compounds, because whereas $[\text{PPh}_4][\text{Fe}_3(\text{CO})_{11}(\mu\text{-Hg}m)]$ solutions are stable at room temperature, $[\text{PPh}_4][\text{Mn}_3(\text{CO})_{12}(\mu_3\text{-H})(\mu\text{-Hg}m)]$ solutions decompose above -10°C .

2.2. Electrochemical behaviour of $[\text{PPh}_4]_2\{[\text{Mn}_3(\text{CO})_{12}(\mu_3\text{-H})]_2\text{Hg}\}$

Under non-stationary conditions in the dichloromethane potential range, no reduction step was observed for $[\text{PPh}_4]_2\{[\text{Mn}_3(\text{CO})_{12}(\mu_3\text{-H})]_2\text{Hg}\}$ (**6**) but two

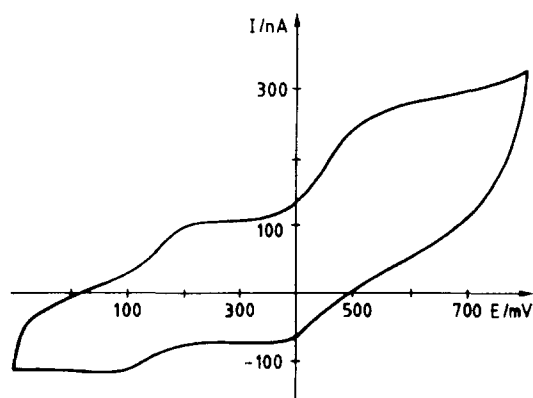


Fig. 4. Cyclic voltammogram of compound **6** in dichloromethane at 50 V s^{-1} showing the two quasi-reversible oxidation waves.

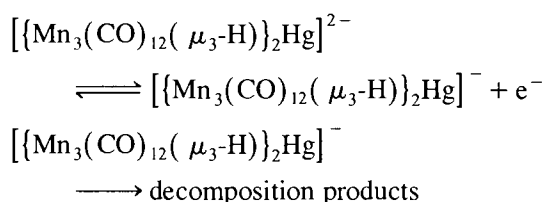
Table 3
Cyclic voltammetry data for compound **6** in dichloromethane 0.1 M $[\text{nBu}_4\text{N}][\text{PF}_6]$ at 50 V s^{-1}

Step	E^0 (V)	$E_{p,a} - E_{p,c}$ (mV)	$i_{p,c}/i_{p,a}$	n
1	0.17	62	0.72	1
2	0.46	133	0.80	2

oxidation waves were observed, at 0.17 and at 0.41 V (Fig. 4). They were both quasi-reversible with $i_{p,c}/i_{p,a} = 0.8$ at 50 V s^{-1} (Table 3). The electron-transfer rate constant k^0 for the first step was 0.26 cm s^{-1} and the α transfer coefficient 0.7. The radical species formed were not detected by EPR spectroscopy, probably because of their short lifetime.

Under stationary conditions, a study of the limiting current versus the square root of the electrode rotating speed showed a deviation from linearity indicating a diffusion-controlled process. Some passivation phenomena occurred on the second wave, precluding further studies.

Controlled-potential electrolysis for the first step consumed 1F per mole of complex. The IR spectrum of the oxidized sample showed the same bands as for the oxidized products of $[\text{PPh}_4][\text{Mn}_3(\text{CO})_{12}(\mu_3\text{-H})(\mu\text{-Hg}m)]$, which were not identified. We therefore propose that complex **6** is oxidized in the first step at 0.17 V according to the equation below.



The monoanion was not stable. Decomposition occurred, leading to products which were not isolated or characterized.

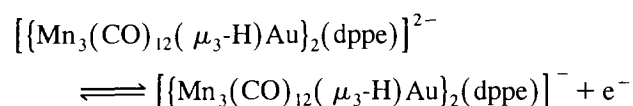
From a comparison between complexes **1–5** and **6**, the influence of the negative charge on the clusters on both the oxidation and reduction potentials is apparent. Thus, the double charge on **6** makes it more prone to lose electrons than **1–5**, but, at the same time, more reluctant to accept them. This idea is strengthened by the fact that the analogous complexes $[\{\text{Ru}_3(\text{CO})_9(\mu_3\text{-}\eta^2\text{-C}\equiv\text{C}^t\text{Bu})\}_2\text{Hg}]$ and $[\text{Ru}_3(\text{CO})_9(\mu_3\text{-}\eta^2\text{-C}\equiv\text{C}^t\text{Bu})\text{Hg}(\text{Mo}(\text{CO})_3\text{Cp})]$ [2b] show very similar electrochemical reduction values due to their zero charge.

2.3. Electrochemical behaviour of compounds $[\text{PPh}_4]_n\{[\text{Mn}_3(\text{CO})_{12}(\mu_3\text{-H})\text{Au}]_n(\text{phosphine})(\text{AuCl})_{3-n}\}$

Given the isolobal relationship between $\text{Hg}m^+$ and AuPR_3^+ [9], it is of interest to investigate complexes containing the metal fragment Mn_3Au , in order to compare the electrochemical behaviour with that found in clusters **1–6**. In addition, our studies were focused

mainly on compounds containing triphos (Fig. 1) in order to determine the possible electronic interaction between the metal fragments through the phosphines. The complexes investigated were $[\text{PPh}_4]_2[\{\text{Mn}_3(\text{CO})_{12}(\mu_3\text{-H})\text{Au}\}_2(\text{dppe})]$ (7) and $[\text{PPh}_4]_n[\{\text{Mn}_3(\text{CO})_{12}(\mu_3\text{-H})\text{Au}\}_n(\text{triphos})(\text{AuCl})_{3-n}]$ [$n = 1$ (8), 2 (9), 3 (10)].

In dichloromethane $[\text{nBu}_4\text{N}][\text{PF}_6]$ at -10°C , the cyclic voltammogram of $[\text{PPh}_4]_2[\{\text{Mn}_3(\text{CO})_{12}(\mu_3\text{-H})\text{Au}\}_2(\text{dppe})]$ (7) showed one quasi-reversible oxidation peak at 0.10 V and a further oxidation peak at 0.73 V (Table 4), but no reduction peak was detected before reduction of the solvent. Controlled potential electrolysis at 0.30 V showed that 1 F is transferred per mole of complex. Although some passivation or subsequent chemical reaction could not be ruled out, we conclude that the first electrochemical step that occurs at 0.10 V is as shown.



This is followed by a cleavage of the monoanion. The species generated could not be isolated or identified.

In THF with $[\text{nBu}_4\text{N}][\text{BF}_4]$ as supporting electrolyte, on a Pt disk electrode at 0.1 V s^{-1} compound 7 exhibited two oxidation processes with a quasi-reversible wave at 0.36 V and an irreversible wave at 1.0 V. The shift in potential values between dichloromethane and THF is probably due to solvent interaction and the same mechanism may occur in both solvents. In the cathodic range, the cyclic voltammograms showed an irreversible wave at -1.69 V of relative intensity 2:1 versus the anodic wave, very similar to compounds $[\text{PPh}_4]_n[\{\text{Mn}_3(\text{CO})_{12}(\mu_3\text{-H})(\mu\text{-Hgm})\}]$. Coulometry at -1.75 V at -10°C was slow and the number of electrons could not be calculated unambiguously. $[\text{Mn}(\text{CO})_5]^-$ was the only compound from the resulting brown solution observed in the carbonyl range of the IR spectrum, and the anionic species generated may have been unstable and decomposed.

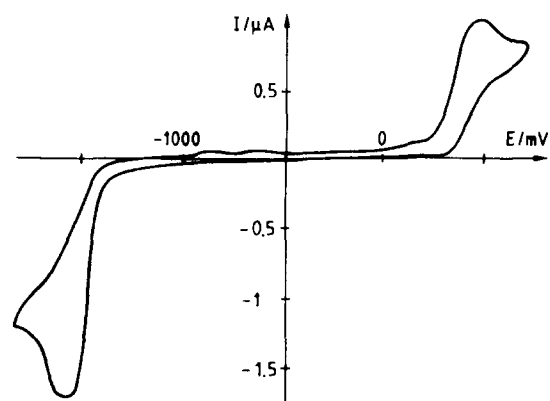


Fig. 5. Cyclic voltammogram of compound 9 in THF at 0.1 V s^{-1} .

Similar behaviour was observed for complexes 8–10 for the oxidation and reduction steps (Table 5, Figure 5). The irreversible second oxidation step appeared at 1.0 V for all of them and was not further studied. The first oxidation peak became quasi-reversible at higher scan rates (at 1 V s^{-1} the intensity ratio $i_{p,c}/i_{p,a}$ is 0.45 and at 50 V s^{-1} is 0.8 on an Au ultramicroelectrode). The E° values are shown in Table 5. The electron-transfer rate constant k° determined by the Nicholson and Shain method [6] using a Technic ultramicroelectrode is approximately $10^{-1} \text{ cm s}^{-1}$ and the transfer coefficient 0.45. The linear voltammograms at a rotating Pt disk electrode showed some passivation phenomena. The study of the limiting current as a function of the square root of the electrode rotation speed showed a deviation from linearity corresponding to a diffusion-controlled process.

Controlled-potential electrolyses were carried out at 0.7 V. Due to some passivation phenomena or to a subsequent chemical reaction, the number of electrons transferred in the oxidation step was not determined unambiguously. The electrolysis data and the following observations indicate that one electron is transferred per Mn_3Au unit: (i) the peak potential values are nearly the same for all compounds (although they have different

Table 4

Cyclic voltammetry data for compound 7 in dichloromethane $0.1 \text{ M } [\text{nBu}_4\text{N}][\text{PF}_6]$ and THF $0.1 \text{ M } [\text{nBu}_4\text{N}][\text{BF}_4]$ at (a) 50 V s^{-1} and (b) 0.1 V s^{-1}

	E° (V) ^a	$E_{p,a} - E_{p,c}$ (mV) ^a	$i_{p,c}/i_{p,a}$ ^a	$E_{p,o2}$ ^b	$E_{p,r}$ ^b
CH_2Cl_2	0.10	65	0.87	0.73	–
THF	0.36	70	0.86	1.0	–1.69

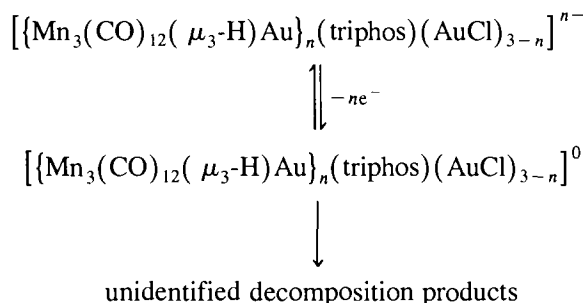
Table 5

Cyclic voltammetry data for compounds 8–10 in THF $0.1 \text{ M } [\text{nBu}_4\text{N}][\text{BF}_4]$

Compound	E° (V) ^a	$E_{p,a} - E_{p,c}$ (mV) ^a	$i_{p,c}/i_{p,a}$ ^a	n	$E_{p,r}$ ^b	n
8	0.41	65	0.91	1	–1.71	2
9	0.41	119	0.76	2	–1.66	4
10	0.35	145	0.88	3	–1.62/–1.68	6

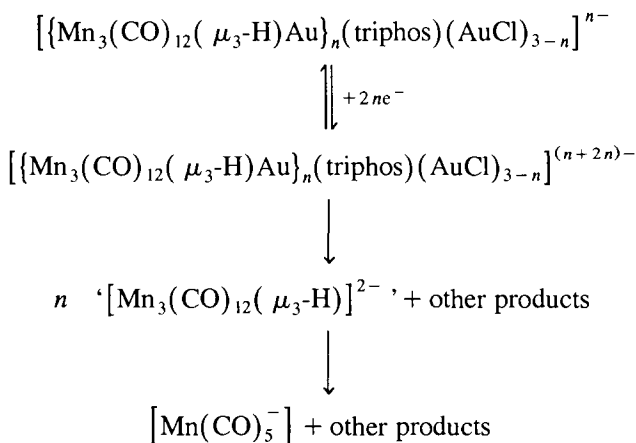
Working electrode: ^a Au electrode ($r = 125 \mu\text{m}$) at 50 V s^{-1} ; ^b Pt electrode ($d = 1 \text{ mm}$) at 0.1 V s^{-1} .

charges); (ii) for compounds **9** and **10**, the oxidation wave at 50 V s^{-1} probably contains at least two electrochemical steps [the ($E_{p,a} - E_{p,c}$) values are very high]; and (iii) the IR spectra of the oxidized solutions are the same in all cases, although the species generated could not be identified. We suggest complexes **8**, **9** and **10** are oxidized according to the scheme below.



The oxidation potentials are somewhat lower than those found for clusters **1–5**, suggesting that the Au–phosphine⁺ fragments are less electron withdrawing than Hg^{m+} units. This is consistent with the increase in the carbonyl stretching frequencies in going from complexes **7–10** to **1–6**. Similar observations have been made for the series of complexes $[\text{Fe}_2(\text{CO})_8(\mu\text{-M})]^-$ (M = Hg^m [10]; AuPPh₃ [11]) or $[\text{Fe}_3(\text{CO})_{11}(\mu\text{-M})]^-$ (M = Hg^m [2c]; AuPPh₃ [12]).

The reduction is irreversible and in the case of **10** there appear to be two mixed peaks. The presence of additional anodic peaks in the reverse scan at 1 V s^{-1} suggests that chemical reactions occur after reduction. One of these was attributed to oxidation of $[\text{Mn}(\text{CO})_5]^-$ by comparison with the voltammogram of an authentic sample, and with literature data [7a,b]. After controlled-potential electrolysis only this species, identified by its IR spectrum, remained. The electrolysis was slow and chemical reactions may have taken place, so the number of electrons was not determined unambiguously but was probably two electrons per Mn₃Au unit (Table 5). In addition, from the cyclic voltammograms, the number of electrons transferred in this step is twice that involved in the oxidation step. Based on these results, the following mechanism is proposed.



As a conclusion from these studies, the first observation that the oxidation peak potential values are nearly the same for all compounds although they have different charges, together with the fact that the reduction potentials are also very similar for all these compounds, indicates that the electrons involved in these processes are delocalized over the metal skeleton, as found for the series $[\text{PPh}_4][\text{Mn}_3(\text{CO})_{12}(\mu_3\text{-H})(\mu\text{-Hg}^m)]$ and $[\text{PPh}_4][\text{Fe}_3(\text{CO})_{11}(\mu\text{-Hg}^m)]$ [2c], consistent with the isolobal analogies between the fragments Hg^m+ and AuPR_3^+ .

The potential difference ($E_{p,a} - E_{p,c}$) increases from **8** to **10** (Table 5) suggesting that the electrochemical waves reflect more than one process, so that a weak interaction among the Mn₃Au units may exist. These compounds would then be an intermediate case if compared with the recently described metal μ -phosphine complexes [13]. For example, $[(\text{CO})_2(\eta\text{-C}_5\text{H}_4\text{Me})\text{Mn}(\mu\text{-dppm})\text{Mn}(\eta\text{-C}_5\text{H}_4\text{Me})(\text{CO})_2]$ exhibits two one-electron waves whereas *trans*- $[\text{PtCl}_2\{(\mu\text{-dppm})\text{Mn}(\eta\text{-C}_5\text{H}_4\text{Me})(\text{CO})_2\}_2]$ (where the central PtCl₂ unit does not permit electronic interaction between the two manganese appendices) shows a single two-electron wave corresponding to an oxidation of Mn^I to Mn^{II}.

3. Experimental details

Compounds **1–6** [4] and **7–10** [5] were prepared as described previously. Electrochemical measurements were carried out with an Electrochemat potentiostat [14] using the interrupt method to minimize the uncompensated resistance (IR) drop. Electrochemical experiments were performed at -10°C in an air-tight three-electrode cell connected to a vacuum argon/N₂ line. The reference electrode consisted of a saturated calomel electrode (SCE) separated from the non-aqueous solutions by a bridge compartment. The counter electrode was a spiral of ca. 1 cm^2 apparent surface area, made of Pt wire 8 cm in length and 0.5 mm in diameter. The working electrode was Pt (1 mm) for cyclic voltammetry, a rotating disk electrode of Pt or Au disk with a diameter of 2 mm and Pt (100 μm) or Au (125 μm) for ultramicroelectrode voltammetry. For electrolysis experiments, a Pt gauze or foil was used. The supporting electrolytes were $[\text{nBu}_4\text{N}][\text{PF}_6]$ (Fluka electrochemical grade) used as received when CH₂Cl₂ was used and $[\text{Bu}_4\text{N}][\text{BF}_4]$ melted under vacuum prior to use for the THF solutions. All solutions measured were $0.5\text{--}1.0 \times 10^{-3} \text{ M}$ in the organometallic complex and 0.1 M in supporting electrolyte. Under the same conditions ferrocene is oxidized at $E^\circ = 0.42 \text{ V}$ (CH₂Cl₂) and $E^\circ = 0.63 \text{ V}$ (THF) vs. SCE. A special electrolysis cell allowing combined coulometry–EPR studies was used [15].

Acknowledgements

Financial support for this work was generously given by the DGICYT (Spain) through Grant No. PB93-0766. G.S. thanks the Ministerio de Educación y Ciencia for a scholarship and for financing her stay in the Toulouse Laboratory of the CNRS.

References and note

- [1] P. Lemoine, *Coord. Chem. Rev.*, **83** (1988) 169.
- [2] (a) P. Lemoine, A. Giraudeau, M. Gross and P. Braunstein, *J. Chem. Soc., Chem. Commun.*, (1980) 77, and references cited therein; (b) D. Osella, L. Milone, S.V. Kukhareno, V.V. Strelets, E. Rosenberg and S. Hajela, *J. Organomet. Chem.*, **451** (1993) 153; (c) R. Reina, O. Rossell, M. Seco, D. de Montauzon and R. Zquiak, *Organometallics*, **13** (1994) 4300.
- [3] See, for example, (a) V.G. Albano, R. Aureli, M.C. Iapalucci, F. Laschi, G. Longoni, M. Monari and P. Zanello, *J. Chem. Soc., Chem. Commun.*, (1993) 1501; (b) L.N. Ito, A.M.P. Felicissimo and L.H. Pignolet, *Inorg. Chem.*, **30** (1991) 988, and references cited therein.
- [4] O. Rossell, M. Seco, G. Segalés, S. Alvarez, M.A. Pellinghelli and A. Tiripicchio, *Organometallics*, **13** (1994) 2205.
- [5] O. Rossell, M. Seco and G. Segalés, *J. Organomet. Chem.*, in press.
- [6] R.S. Nicholson and I. Shain, *Anal. Chem.*, **36** (1964) 706.
- [7] (a) D.A. Lacombe, J.E. Anderson and K.M. Kadish, *Inorg. Chem.*, **25** (1986) 2074; (b) G. Pampaloni and U. Koelle, *J. Organomet. Chem.*, **481** (1994) 1; (c) K.M. Kadish, D.A. Lacombe and J.E. Anderson, *Inorg. Chem.*, **25** (1986) 2246; (d) M. Tilset, *Inorg. Chem.*, **33** (1994) 3121.
- [8] The nucleophilicity of many carbonylmetallate anions has been established by comparison of their relative rates of reaction with alkyl halides. Thus, from the reaction $m^- + RX \rightarrow m - R + X^-$, it is possible to obtain k_2 , the pseudo-first-order rate constant. With $k'_2 = k_2 / k_{2(CO)}$, k'_2 values for each organometallic fragment have been estimated: R.E. Dessy, R.L. Pohl and R.B. King, *J. Am. Chem. Soc.*, **88** (1966) 5121.
- [9] J.W. Lahuer and K. Wald, *J. Am. Chem. Soc.*, **103** (1981) 7648.
- [10] R. Reina, O. Rossell and M. Seco, *J. Organomet. Chem.*, **398** (1990) 285.
- [11] O. Rossell, M. Seco and P.G. Jones, *Inorg. Chem.*, **29** (1990) 348.
- [12] O. Rossell, M. Seco, R. Reina, M. Font-Bardía and X. Solans, *Organometallics*, **13** (1994) 2127.
- [13] P. Braunstein, M. Knorr, M. Strampfer, Y. Dusausoy, D. Bayeul, A. DeCian, J. Fischer and P. Zanello, *J. Chem. Soc., Dalton Trans.*, (1994) 1533.
- [14] P. Cassoux, R. Dartiguepeyron, C. David, D. de Montauzon, J.B. Tommasino and P.L. Fabre, *Actual. Chim.*, **1** (1994) 49.
- [15] G. Cros, J.P. Costes and D. de Montauzon, *Polyhedron*, **3** (1984) 585.